Experimental Realization of Deadbeat Control on a Hybrid Model of Legged Locomotion

Tianqi Li

A thesis
submitted in partial fulfillment of the
requirements for the degree of

Master of Science in Mechanical Engineering

University of Washington

2018

Reading Committee:

Samuel A. Burden, Chair

Sawyer B. Fuller

Eric Rombokas

Program Authorized to Offer Degree:
Mechanical Engineering

University of Washington

Abstract

Experimental Realization of Deadbeat Control on a Hybrid Model of Legged Locomotion

Tianqi Li

Chair of the Supervisory Committee:
Assistant Professor Samuel A. Burden
Department of Electrical Engineering

In this thesis work, I validate the deadbeat controller on a one-legged hopper by experiment, which includes the construction of the test bed, controller build-up, adjustment of dynamics for the controller and experimental validation for the controller. The mechanical test bed is designed and built for the one dimensional hopping experiment with changing terrain to validate the deadbeat controller. The deadbeat controller is generated by parameter optimization on the Poincaré Map, which is provided by [9] based on the analysis of running animals whose dynamics can be partially or fully controlled by the encoded control laws in the feedforward trajectories of the appendages. The controller is able to achieve deadbeat stability of the apex by controlling the dynamic with only sensing of apex heights. Based on dynamics of the hopper, the method of decreasing energy dissipation is applied that is to attach springs on the leg. By exploring the hopper, the return map of terrain disturbance and control input is measured in physical experiment. Finally the controller is validated on the experiment of hopping on the changing terrain with small terrain feedback sensing.

TABLE OF CONTENTS

LIST OF FIGURES

LIST OF TABLES

ACKNOWLEDGMENTS

First and foremost I want to express the deep and sincere gratitude to my advisor, Prof. Samuel Burden, for receiving me into his group when I entered UW, teaching me control system and reinforcement learning. As my advisor, he offered thoughtful help to my thesis, including making suggestions to experiments, communicating with Prof. Shai Revzen and Dr. George Council in University of Michigan who remotely hear updates of this thesis. And thanks Sam for supporting my PhD application!

Sincere appreciation to all my fellow labmates in BRL, where I had a great time in these two years. This is a warm place everybody helps each other in study and life. In particular, I want to thank Andrew who keeps great patience for guiding my work, Liam who started thesis together with me and end together, Yana and Jake for their former construction of our test bed, Prof. Blake Hannaford for supporting my PhD application and his expectation to me, Bora, Mammona and Shruti for giving me advice on my study and application. My completion of this project could not have been accomplished without the support of you!

Specially I would like to thank Prof. Sawyer Fuller, my committee member. My motivation of robotics came from his class Bio-inspired Robotics, where he introduced to the study of robotics to me. And I'm grateful to his support for my PhD application!

Very fortunately our test bed was moved to AMP lab, where I shared the room with group of Prof. Eric Rombokas. I want to thank the lovely people for bearing my hopper's noise and encouragement to me.

Special mention goes to friends who studied with me during the two years in UW (Dizhi, Zhenyu, Tina, Weichen, Yang, Junlin, Nan, Fangzhong, Yanjun, Jingyun). They extended my knowledge, and kept me not being alone.

To my parents Xiaohong and Bing, who gave me the chance to do everything on this planet including this paper. I owe it all to you!

DEDICATION

to Muxi, who wants to purchase my robot

Chapter 1
INTRODUCTION

This chapter briefly summarizes the problem to be addressed in this thesis, and the work accomplished to solve the problem.

1.1 Running locomotion

Legged locomotion is an important part of robotics. In legged locomotion system, this hybrid system has dynamic behavior transition during and after impact on the ground, which coincides with the loss of control authority driven by the disturbance externally. To behave adequately to accomplish a given task, robots are ought to overcome disturbance from the environment [4], and legged locomotion is particularly affected by the unpredictable terrain.

In legged locomotion, running is the locomotion requires stability [6]. The reason includes several points, first to make continuous upper limb motion, adequate time is required in the air. Second, the stability in running includes periodicity [6]. Unlike jumping for distance, the pattern in running is periodic motion of limb, and stability is the consequent goal in running locomotion. Thirdly, from the hypothesis in [13], running in periodic way has the benefit of decreasing the computational burden for animals by triggering the feedforward controlling of limbs. To deal with the uneven terrain to keep stability while running, legged animals have the feedforward mechanism to overcome uneven terrain. The research found in [35] points out more energy is consumed in running on uneven terrains by measuring metabolic energy. With the measurement of EMG, the decrease of ankle joint work is found in running in uneven terrain, which is explained by understanding that muscles at the distal joints rely on high-gain proprioceptive feedback [10], while the more proximal knee and hip joints are largely feed-forward controlled. Also in [32], a 'swing-leg retraction' is observed

that in human's running the leg swings to the front prior to touchdown, and moves the foot reward towards the ground. This mechanism is simulated in a SLIP model which leads to the conclusion of the swing-phase limb dynamics may play an important role in the stabilization of running animals. Last but not least, the change of leg stiffness plays the role in adapting the speed changes in running to increase the stability in different angle of attack [20].

1.2 Current state of Research

To make horizontal transportation on the ground, wheel is the most efficient method in human's engineering system: wheels convert the speed of motor direct to velocity on the ground; unlike leg, wheels avoid impacts on the ground which causes energy dissipation. However, to make wheeled machine running great civil engineering has to be achieved for building roads. Machines are supposed to work with mobility not only on plain road but also on rough terrains, like running on grassland or hopping upstairs. To fully interact with environment, robots with legged structures are designed to overcome different terrains.

One main technique for robots to overcome terrain is visual feedback, including big dog [25] and [11]. With 3-D mapping, the locomotion planning is applied to adjust the terrain. While in running locomotion, mapping and motion planning is too slow to keep continuous movement. Moreover, the terrain's change requires remapping of the system.

To keep the pace, controller in running is supposed to behave more feedforward, [13] points out the hypothesis that the neural control of running locomotion is a more mechanical and feedforward way with less sensing and positive adjustment of the terrain feedback. This feedforward control is studied by SLIP model by [32]. The robot with trajectories of SLIP includes RHex robot [1]. Simulations of control with SLIP model include [9, 23, 26], yet the experimental validation of the controller is rarely presented to physically realize this model based control. In this thesis, the main propose is to physically realize the control on one SLIP modeled robot.

1.3 Objectives

The following objectives are set for this thesis:

- To construct the experimental setup for simulating the terrain disturbance to the 1-dimensional hopper.
- To precisely control the hardware setup and sensing system.
- To build the deadbeat controller based on the hardware system.
- To validate the deadbeat controller by the result of experiment.

1.4 Summary of Contributions

In this thesis with the goal of experimentally validating the deadbeat controller on the running legged locomotion, the work is divided into the following sections:

1. Design, fabrication and assembling for horizontal 1-D linear test bed.
2. Digital control of the test bed and hopper.
3. Explore the hopper's dynamics under terrain disturbance.
4. Build the deadbeat controller and experiment.

Based on our topic, we need to provide uneven terrain for the robot, and I **design, fabricate and assemble** one 1-D horizontal test bed, which was used for carrying different terrains while the robot is hopping upon the terrains. This hardware setup provides stable position of the terrain under the condition of small disturbances from hopping impact. The test bed is built based on a linear guide and bearing carriage, and the power train includes one brushless direct driven motor and chain drive.

Using PD controller, the motor and horizontal test bed are controlled to provide continuous hopping and terrain changing. The promising performance of **digital control** on the hardware makes the deadbeat controller applicable on the hardware.

To build up the deadbeat control, I **explore the dynamics** of the hybrid system by measuring hopper's body and foot positions under uneven terrains. And to build the controller, the PD parameters are used as the output of the deadbeat controller.

Finally, the **validating experiment** is conducted by controlling the hopper with terrain information input to the deadbeat controller in real-time. The sensing of the apexes height is captured by the real-time date in Qualisys Motion Capture System SDK, which is sent to motor's encoder in C++ to perform deadbeat control.

As the main aim of this thesis, a deadbeat controller is implemented to keep constant apex to different ground levels which are used as the simulation of uneven terrain. The result shows the controller decreases the time steps to converge to desired apex for terrain change within ± 3 cm.

1.5 Organization of the Thesis

This thesis work is divided into four parts which is presented in detail at the following sections. Chapter 2 makes brief introduction of the locomotion and control, including the basic model hybrid dynamic system, the widely used SLIP model in running locomotion, the periodicity in locomotion and the definition of deadbeat.

The second part in chapter 3 is the brief introduction of hardware in related experiment: 1-dimensional hopper, the test bed and camera. Then follows the method of controlling the hopper and test bed.

The third part presents the details of dynamics exploration on the hopper. To explore the hopper whose model is not mathematically determined, chapter 4 introduces the experiment which observes the subsequent dynamic of hopper after terrain disturbance.

The last part, in chapter 5, is the design and experimental validation of one deadbeat controller on the hopping apex under terrain disturbance. First, a mathematical controller

is given by Poincaré return map. Then by varying the controlling parameter, a return map is obtained. Finally a controller is built and the experiment is conducted. Result analysis in the validating experiment shows the different dynamics between open loop control and the controller. As a conclusion, the controller improves the stability of the hopper to reject terrain disturbance.

Chapter 2
BACKGROUND

This chapter introduces the theoretical background of the running locomotion. In running locomotion, the inconsistency of dynamics happens when hopper touches or leaves ground, and this is the feature of hybrid dynamics system in section 2.1. The basic concept of SLIP model is presented in section 2.2 which is widely studied in running locomotion. In running, the periodicity is tight with the stability of the system, with the utilization of Poincaré map to analyze the system in section 2.3. Section 2.4 lists the definition and feature of deadbeat control.

2.1 Hybrid Dynamic System

In many dynamic systems, for example jumping and running, both continuous-time and discrete-time dynamics are included in the system [15, 16]. For continuous dynamical behavior like ballistic dynamics and stance dynamics, the position and velocity of the robot change continuously according to the Newtons second law. But impact happens at the touchdown point, which instantaneously makes the velocity of the toe directly to zero, and the discrete change happens.

To express the continuous and discrete model, a widely used mathematical model is used. In continuous-time dynamics, with x an Euclidean space R^n representing the current state of the system, the first-order differential equation is

$$\dot{x} = f(x), \tag{2.1}$$

and $x \in C$, C is the subset of the R^n. And in discrete system, the typical model is the first-order equation

$$x^+ = g(x), \tag{2.2}$$

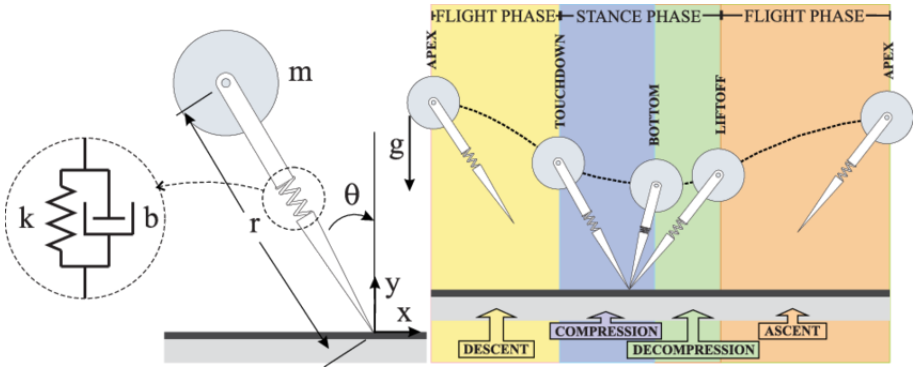

Figure 2.1: The SLIP Model. (a) Coordinates and model parameters. (b) Locomotion phases (shaded regions) and transition events (boundaries) [3].

with $x \in D$ and $D \in R^n$, this indicates the next value of the state is given as the function of current state x by function $g(x)$. c, D are the subset for continuous and discrete which are all subset of R.

In hybrid system, given the function $f(x)$ and $g(x)$, and the initial state value x_0, the system could be solved by integration.

2.2 Spring Loaded Inverted Pendulum Model

The Spring Loaded Inverted Pendulum (SLIP) is used as the model of running legged animals and robots, which is firstly introduced in [13]. The trajectory of the COM is accurately interpreted in this spring-mass model [7, 12]. In [31] and [14], the SLIP model is found to have 'self-stability' gaits in running. With the study in human running [32], a SLIP model is applied to simulate with positive result of 'swing-leg retraction' feedforward control. Not only sagittal plane, the SLIP model is studied in 3 dimensional space [29].

In SLIP, a hybrid system, the dynamics and derivation of the state is divided by events, which is touchdown and lift-off. At touchdown, the transition between air to stance happens. The toe part loses the velocity, and part of the system's energy is dissipated. At lift-off, the toe is lifted with the loss of contact to ground, and the leg drags the toe leaves the ground.

After lift-off, COM will reach the highest point of the trajectory which is the apex.

2.3 Periodicity

In the running locomotion, the dynamics of the system could be considered in the beginning and end of the strides, with the state at beginning of kth stride p_k to the beginning of next state of stride p_{k+1}. Because running locomotion is a hybrid dynamic system, the flow of the state is separated by events which the dynamic changes, and in running the dynamic domains mainly includes descent, stance, and ascent as Fig 2.1 shows. In the running locomotion where state $p \in R^d$,the non-trivial way of describing the dynamics between p_k to p_{k+1} is

$$p_{k+1} = \Phi_{ascent}(\Phi_{stance}(\Phi_{descent}(p_k, \tau_{descent}), \tau_{stance}), \tau_{ascent}). \tag{2.3}$$

where $\tau_{descent}, \tau_{stance}, \tau_{ascent}$ is the time in descent, stance and ascent domain, and $\Phi : R^d \times R \to R^d$ which is the flow in different dynamics.

To judge if the system reaches the steady state running, the following two requirements are supposed to satisfy [27]:

1. The beginning of stride state x_{k+1} is achieved by the last stride x_k with some motion;

2. All strides have same state at the beginning state $p_{k+1} = P(p_k, l) = p_k$.

In the second requirement, the function $P(p_k, l)$ is the Poincaré function which maps the state p_k on a lower-dimensional subspace, called Poincaré section S, to the next state p_{k+1} on section S, and l is the set of all inputs includes disturbance and control during the stride.

2.4 Deadbeat Control

Deadbeat control is the control that drives the state of the system to the steady state in the smallest number of time steps, which is widely applied in discrete-time system . In a Nth - order linear system, feedback is able to apply to make all poles of the closed-loop transfer

function of the state to the origin. And a linear feedback with no more than N number of steps is able to make the system achieve the steady states [17].

A deadbeat controller has the response with features:

1. zero steady-state error;

2. minimum rise time; minimum settling time;

3. <2% overshoot;

4. high control signal output.

Chapter 3
HARDWARE SETUP

This chapter presents the details of hardware for the one-legged locomotion experiment. The hardware includes one dimensional hopper, test bed for the hopper, optical system and terrain. Section 3.1 details the one-legged hopper we used in the experiment. Section 3.2 presents the mechanical design, digital control of the test bed built to meet the prerequisite of the experiment. Section 3.3 describes the optical system in our lab to help us capture the trajectories of the hopper. Section 3.4 introduces the terrain designed to test the stability of deadbeat controller.

3.1 Hopper

3.1.1 Mechanical Structure

The hopper is designed and built by Ghost Robotics LLC [19], and it is actually one leg of this companys four legged robot Minitaur [18]. As fig. Shows, it has the quadrilateral shape of the leg, with 2 degree of freedoms (DOF) driven by 2 direct-driven (DD) motors. The motors are Tiger Motor U8-16 100kV U-Power Professional Motor. The benefits of using the DD motors for legged locomotion include three points [18]. First DD motor has higher transparency, backlash, viscous friction from the gearbox could be avoided. Second without gearbox, DD motor provides better mechanical performance of the robot due to the decreasing of the inertia, as the usage of N:1 gearing causes N^2 increase on the inertia [24]. And also DD motor improves the energy efficiency of the system because of no loss of the energy to the gearbox. Third, DD motor enhances the sensing system by mitigating the low-pass spring-mass dynamics in series elastic actuators (SEA), which avoids the low-pass filtering of actuation signals[24].

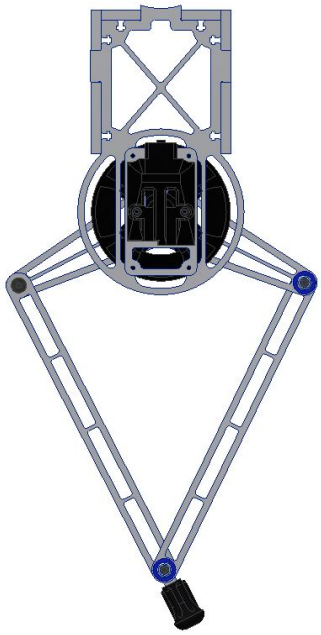

Figure 3.1: The CAD model of the one-legged motor

Except for the motor, the design of the hopper with a symmetric five-bar linkage brings the advantage in higher proprioceptive sensitivity $\sigma_m in$, higher force production $\sigma_m ax$ and less thermal cost of force $\sigma_m ean$ than the Open-chain design and parallel five-bar design in Fig 3.1. Also in the symmetric five-bar linkage leg design, larger workspace, the angle range of the upper leg, brings the 2.1x energic output and 5x decreases in energy loss of touchdown impact when comparing with the conventional design [18, 19].

3.1.2 Control Method

The hopper is controlled by the MBM mainboard with Ethernet cable port, which is provided by Ghost Robotics LLC. MEM mainboard is programmed in C++ language. The encoder in motor provides the angular position and velocity of the motor, and it supports two ways of driving the motor, PWM (Pulse Width Modulation) and PD positioning control.

PWM method is to use digital signal to control power applications by controlling the

width of the pulses, the function to call PWM is getOpenLoop(PWM) , and the raw PWM value is between $[-1, 1]$. In PWM mode, the hopping motion could be implemented in Algorithm 1.

Algorithm 1 PWM hopping

```
1: procedure PWM HOPPING
2: loop:
3:     getOpenLoop(pwm);
4:     delay(time)
```

PD (Proportional Derivative) control is a control loop with feedback, which is widely used in industrial control systems. In the motor's positioning, the PD controller uses the measured position $\theta_{measure}(t)$ and the desired value $\theta_{set}(t)$ to generated the error value $e(t) = \theta_{set}(t) - \theta_{measure}(t)$. Mathematically, the overall PD control function could be expressed as

$$u(t) = K_p e(t) + K_d \frac{de(t)}{dt} \tag{3.1}$$

In this equation K_p and K_d is the proportional and derivative terms. The $u(t)$ in the motor encoder stands for the PWM value, and the PD controller is called by SetGain(K_p, K_d) and SetPosition(θ_{set}) function. The simple way of making hopping by PD control is to set two angles, which we name the contract position θ_1 and extending position θ_2: the hopper keeps contracting position in the air, and switches to extending position after touch down to push the leg leave the ground.

To get hopping with stable pace and desired height, we need to set proper time for the two position as well as proper PD parameters.

3.2 Test Bed

To realize the one-dimensional hopping with changing terrain, the test bed should constrain the hop moving in vertical dimension and a horizontal platform which can provide different

Algorithm 2 PD controller hopping

```
1: procedure PD CONTROLLER HOPPING
2: loop:
3:     contracting position
4:     setGain(K_p1, K_d1);
5:     SetPosition(θ_1);
6:     delay(t_1)
7:     extending position
8:     setGain(K_p2, K_d2);
9:     SetPosition(θ_2);
10:    delay(t_2)
```

terrain. The design is divided into two parts, vertical constraints and horizontal platform.

3.2.1 vertical frame

A frame setup is built in the lab, it consists of:

- 80/20 aluminum frame for support of harness.
- Linear motion guide.
- Steele angles for attaching the hopper to the Linear motion guide.

A ball bearing Linear motion guide was chosen to minimize the friction, and the design and construction of the vertical is from the work of [5] and [34].

3.2.2 Horizontal platform

To change the terrain beneath the hopper, I designed the one dimensional treadmill. Treadmill is widely applied in the robot locomotion and human studies [36, 28, 30], which can

Figure 3.2: The CAD model of the test bed

simulate the running and walking without the effort of creating long routine and long terrain. Similarly, a treadmill is designed and built for the validation experiment of deadbeat controller. As Fig 3.3, the treadmill is designed to carry terrain on its platform, and it could move back and forth to change the terrain when the hopper is in the air, and it should reach the set position before the hopper touches down.

The principle of the treadmill includes

1. *Precision*: The treadmill is supposed to have the ability to move to the set position with the error small enough so that the desired terrain can be delivered under the toe of the hopper.

2. *Agility*: The average time gap between the two touchdowns of the hopper is around 250 ms, and during this period, the treadmill should complete the positioning task, and this requires high agility.

3. *Control signal*: To successfully coordinate the movement of hopping and terrain changing, we need to centralize the control to both treadmill and hopper. To avoid the complexity of the control system, same motor in the hopper is applied to drive the treadmill.

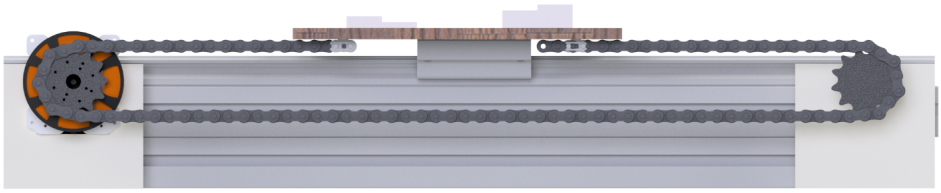

(a) Front view

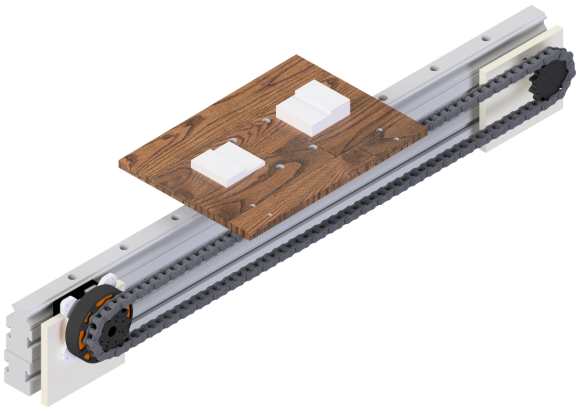

(b) Side view

Figure 3.3: CAD Design of treadmill, rendered picture

A chain drive is designed for the treadmill. Due to the treadmill needs to make precise movement in two directions during a limited time, the belt drive style is not applicable due

to belts deformation as well as belt drive is used at speed of the order of 10 to 60 m/s [22]. Thus the chain drive is selected.

Based on the prepared hardware: One Tiger U8 Motor, one 900 mm linear motion guide. The expected platform length is 30cm, and the maximum velocity for terrain transition is $300mm/0.2s = 1500mm/s$, and for the motor with diameter of d = 80mm, the maximum requirement for motor's frequency of rotation is $n = \frac{1500}{80\pi} = 5.9r/s = 36.4rpm$. The peak power of the motor at 16V is 267W. The center distance between the motor and driven sprocket is approximate $C = 700mm$.

Based on the procedure of roller chain selection in [22], we will pick a single standard chain and sprocket.

1. The poweer to be transmitted: 267 W.

2. the speeds of driving shafts: 30 rpm.

3. The characteristics of driving shaft: with slight shocks, smooth.

4. Approximate centre distance $C = 700mm$.

5. The desired reduction ratio: 1.

6. The application factor from table $f_1 = 1.1$ (with slight shocks), tooth number $N = 18$, tooth factor $f_2 = \frac{19}{N} = 1.05$.

7. Calculate the selection power: selection power $= 267W \times f_1 \times f_2 = 0.31kW$

8. Using the power speed rating charts by manufacturers we can select the chain drive pitch RS 400 18T, the pitch (length between rollers) is $p = 0.5in = 12.7mm$.

9. Calculate the chain length: $L = N + \frac{2C}{p} = 18 + \frac{1400}{12.7} = 128.2pitches$. The nearest even number is L = 128 pitches.

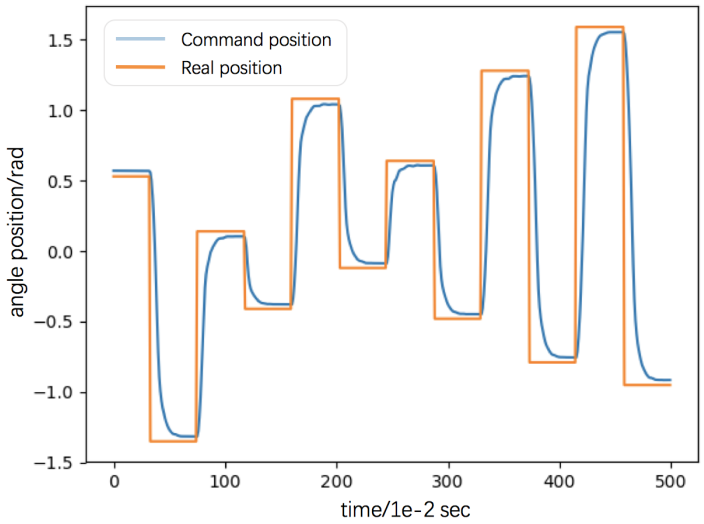

Figure 3.4: Control result of the treadmill, under the PD parameter of $K_p = 0.9, K_d = 0.05$.

10. Calculate the exact centre distance: $C = \frac{p(L-N)}{2} = 55 pitches = 698.5mm$.

With sprocket and chain chosen, the other parts are chosen and designed for supporting the chain and platform. The design and real part is shown in Fig 3.3.

3.2.3 Digital Control

With the horizontal model built, PD positioning control is applied on the motor installed in the treadmill to control the motor. The PD parameter is optimized under the angular position command of the motor in the pattern which tracks the terrain under the order designed for test (see section). The command is changing every 80 ms (half of the hopper's gap time between touchdowns), with DC power 16 V/ 30 A. After the procedure of PD parameter selection, the optimal result is shown in Fig 3.4. The result suggests the treadmill is precise and fast enough to satisfy the prerequisite for changing terrain.

3.3 Optic System

To capture the trajectory of the hopper, an optic system is applied in this experiment, one Qualisys Oqus motion capture camera is used, with the camera directly facing the hopper with the distance of 2.5 m. Oqus camera is connected by host computer by TCP/IP protocol, which is able to capture the position of IR (infrared ray) markers in 2D mode in 1 kHz for offline capture and 100 Hz for reading the data with Qualisys system's real time SDK. To explore the dynamic of the hopper, I attached IR markers on the upper body and toe for measurement.

3.3.1 Calibration

The position of the IR markers is captured in coordinate of pixel by Qualisys camera. To get the trajectory of the markers, transferring pixel into physical world is required. A simple method for camera calibrating is applied in this experiment. As Fig 3.5 shows, to transform the camera's coordinate of P_1 and P_2 IR markers into $\overrightarrow{n_1}O\overrightarrow{n_2}$ coordinate, we need X, Y, O three markers to make $\overrightarrow{n_1}$ and $\overrightarrow{n_2}$. And the transformed coordinates of P_1 and P_2 in $\overrightarrow{n_1}O\overrightarrow{n_2}$ coordinate are

$$P_1\text{:}\ \begin{bmatrix} \mathrm{x}_1 \\ \mathrm{y}_1 \end{bmatrix} = \begin{bmatrix} \frac{\overrightarrow{OP_1}\cdot\overrightarrow{n_1}}{|n_1|} \\ \frac{\overrightarrow{OP_1}\cdot\overrightarrow{n_2}}{|n_2|} \end{bmatrix}$$

$$P_2\text{:}\ \begin{bmatrix} \mathrm{x}_2 \\ \mathrm{y}_2 \end{bmatrix} = \begin{bmatrix} \frac{\overrightarrow{OP_2}\cdot\overrightarrow{n_1}}{|n_1|} \\ \frac{\overrightarrow{OP_2}\cdot\overrightarrow{n_2}}{|n_2|} \end{bmatrix}$$

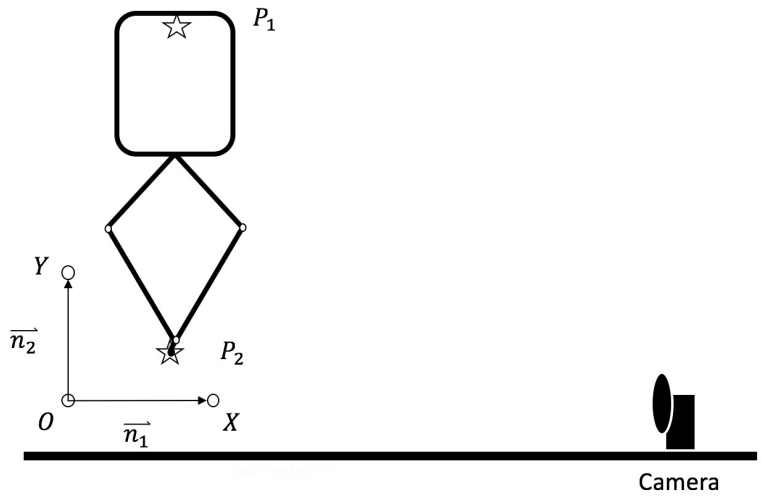

Figure 3.5: Calibrate points in 2D plane.

Chapter 4
DYNAMICS EXPLORATION

With hardware for the experiment prepared, this chapter discovers the dynamics of hopper with open loop hopping on changing terrains. In section 4.1, a physical correction is applied on the hopper to make its dynamic close to a spring-mass model, and hopping with nadir detection is applied to adjust the correction. Section 4.2 describes the experiment of exploring hopper's dynamics under terrain disturbance including experiment method and analysis of dynamic.

4.1 Open Loop Hopping Control

To decrease energy dissipation after impact at touchdown, the hopper is supposed to have the feature of spring-mass system which has several rebounds and the subsequent apex height is exponentially decaying when dropped to the ground. To achieve this dynamic feature, a physical linear spring is attached on the leg (See Appendix A). And a different hopping pattern, nadir detecting hopping, is implemented with the attachment of spring.

4.1.1 Spring Attachment on Hopper

The hopper's basic information is introduced in Section 3.1. To better restore energy and hop higher, a linear spring is attached between the leg. A drop test is conducted to test the effect of energy storage without and with spring. As the Fig 4.1 shows,in the drop test the hopper's leg is set to a fixed angle (30°) by PD controller, and the hopper is dropped from 14 cm above the ground.

With motion capture camera, we recorded the position of the top and toe marker in the drop test. Fig 4.2 is the comparison of top and foot marker's trajectory between the hopper

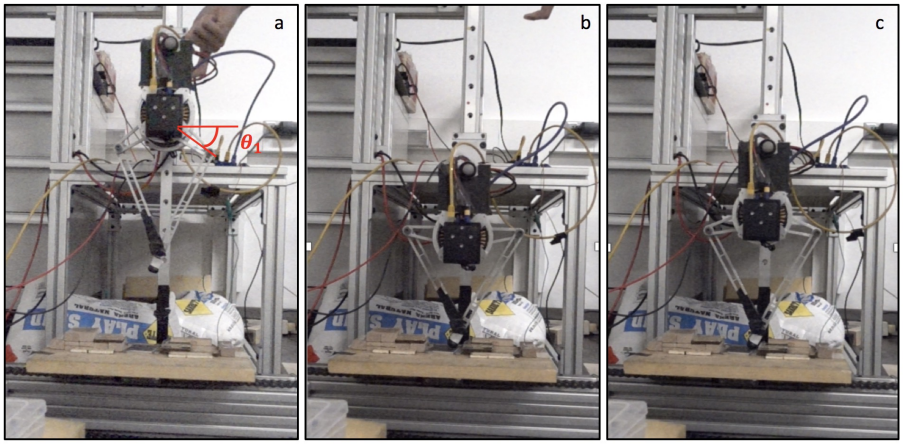

Figure 4.1: Drop test, a) start drop the hopper, the θ_1 marked is angle between hopper's upper leg to horizontal base line, in this case $\theta_1 = 30°$; b) after touch down, θ_1 will decrease due to upper body's weight; c) after top marker's nadir, the hopper will start to bounce up.

with and without spring. From Fig 4.2 b) the foot's trajectory, it shows the hopper has more rebounds with spring attached (4 times the foot rebound in orange line) than without spring (2 times the foot bounces up), which supports that energy is absorbed in the spring after touchdown and injected into the hopper after nadir, which makes the foot leaves the ground 2 more times. Secondly in Fig 4.2 b) the top marker has the subsequent apexes a smoother decaying in the spring-attached hopper, which suggests part of energy is restored in the spring. Third, the natural frequency of a simple spring-mass mechanical system is:

$$f = \frac{1}{2\pi}\sqrt{\frac{k}{m}}.$$

With spring attached, the resonance frequency of the top marker's vertical position oscillation becomes apparently higher than previous system, which shows the feature of the spring-mass system in our hopper.

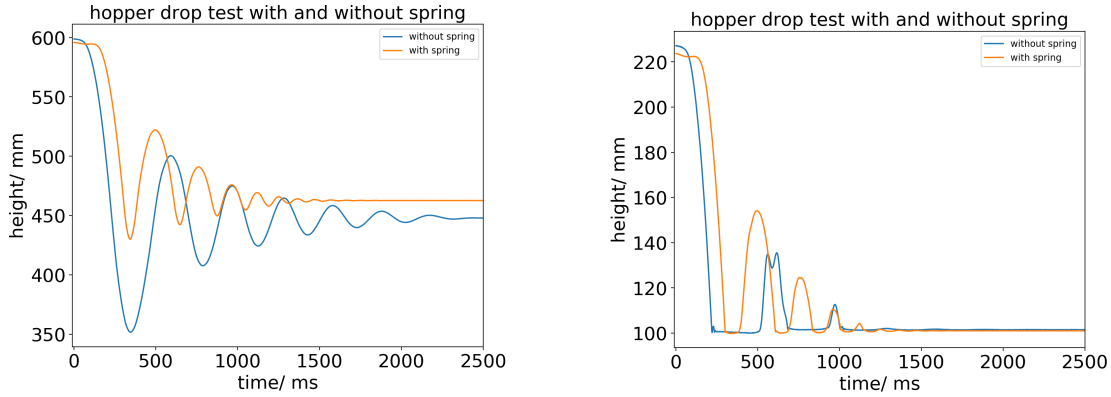

(a) top marker trajectory

(b) foot marker trajectory

Figure 4.2: Captured trajectory of top and foot marker in drop test

4.1.2 Nadir detecting hopping

With spring attached, a new hopping with nadir detection is applied. Because of the spring's mechanical resonance frequency, if we use fixed-time PD positioning command on the hopper (Algorithm 2), the hopper will be very sensitive to terrain disturbance and the hopping will become unstable. Thus a detection of nadir is used to stabilize hopping. The hopper keeps at contract position $\theta_1 = 30°$, and when the robot reaches its nadir, the positioning command of extending position will be triggered to inject energy into the system.

To detect the dynamics of this nadir detection hopping, one hopping test is conducted to test the stability of the nadir detecting hopping. The hopper is set to hop on constant ground height, and hopping apexes are captured by camera. The result shows that the apexes of the hopping is normally distributed, and the hopping is pretty stable with variance of apex height under 1 mm.

4.2 Apex dynamic

This section explores the law of subsequent apexes change caused by terrain change with nadir detecting hopping in section 4.1. The hopper is set to hopping on the test bed, and

Algorithm 3 Nadir detecting hopping

```
1: procedure NADIR DETECTING HOPPING
2: loop:
3:     contract position
4:     setGain(K_p1, K_d1);
5:     SetPosition(θ_1);
6:     if nadir then
7:         extend position
8:         setGain(K_p2, K_d2);
9:         SetPosition(θ_2);
10:        delay(t_2)
```

the terrain is changed ten hops per terrain type (achieving the new steady apex, and the hopper has no information about terrain change. The exploration of this open loop hopping with terrain disturbance demonstrates the stability of the system, which could be utilized as the comparison for the result of the deadbeat controller.

4.2.1 Experiment setup

In the experiment, the hopper is set to hop upon the test bed with different terrains. Tow blocks with height of 10 mm and 30 mm is used as terrain, which can provide terrain height change of ±10 mm, ±20 mm and ±30 mm. The hopper hops ten times on the terrain, then the terrain changes after the 10th hop when the hopper is in the air, meanwhile hopper and test bed's motors' angular positions are logged by USB serial port to host computer. As Fig 4.3 shows, the marker's position data captured by camera is saved in Qualisys software.

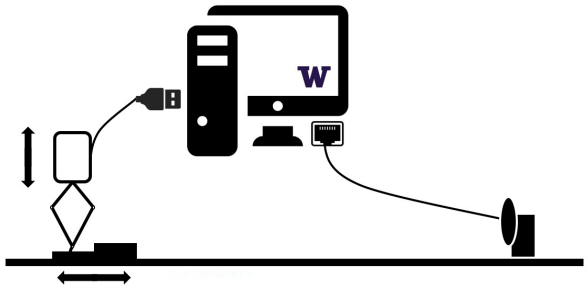

Figure 4.3: Experiment sketch for open loop hopping experiment with terrain change. Hopper is hopping in vertical dimension, and terrain transition happens when the hopper is in the air. Motors in hopper and test bed log data to host computer by USB serial port. Camera captures top and foot IR maker's position in 1k Hz, and the data is saved after experiment and sent to host computer with TCP/IP protocol.

4.2.2 Result analysis

From the top marker's trajectory, all apexes are captured combined with terrain's height information. One method to analyze the dynamics of apex is to observe the apex's change after the terrain transition. In Fig 4.4, the terrain transition happens after apex number 0, the subsequent apexes are scattered on three subplots which are divided by different terrain height change ($\pm$10 mm, $\pm$20 mm and $\pm$30 mm). The apex height h has the trend of converging after the transition, and at 8th or 9th hop, it can be assumed that apex height reaches the new steady state. Between different terrain change, the apex has different speed (number of hops) to reach the steady state. For example, after $\pm$ 10 mm terrain change the apex reaches the steady state at second hop, while the apex takes 2 more hops to achieve steady state after $\pm$ 20 mm and $\pm$ 30 mm terrain change.

Fig 4.4 d) includes all subsequent apexes after terrain change. The statistical apex means $\bar{h}$ and variances σ for each number of apexes are listed in Table 1. From table 4.1, the mean of apexes has minor variation after the terrain disturbance. Due to terrain change in the

experiment is symmetric, for example same number of -10 mm change with +10 mm change, the mean keeps the same with number of hops, and variance is a more direct indicator of apex's stability. In table 4.1, the variance starts at 19.1 mm, and starts decreasing afterwards. In this experiment, the variance threshold 1.5 mm for stable state is set. As a conclusion, the apex starts to reach new steady state after 4 hops in open loop hopping.

Table 4.1: Statics of apexes height h in number of hop after terrain transition in open loop hopping: mean $\bar{h}$, squared deviation σ, p-value of Bartlett test

number of hops	0	1	2	3	4	5	6	7	8	9
$\bar{h}$/ mm	475.3	474.9	474.9	475.1	475.2	475.2	475.2	475.2	475.2	475.2
σ/mm	19.1	8.1	3.5	1.7	1.1	1.1	1.2	1.2	1.4	1.4
p-value	1e-7	2e-5	2e-4	0.03	0.98	0.60	0.70	0.27	0.88	

Additionally, Bartlett test is used to analyze if the apex reaches steady state. In statistics, Bartlett's test [33] is used to test if more than two samples are from populations with equal variances. In this case, the Bartlett test is applied for (kth apex, k+1th apex) to analyze the homogeneity of variances between the two sample of different apexes, if the p-value of Bartlett's test is less than 0.05, we reject the null hypothesis that samples are from populations with equal variances, which means the apex does not reach the steady state after k hops. In table 4.1, the p-values of the Bartlett test for 0th - 8th apexes are listed. The result shows that p-value starts with number smaller than 0.05 which means apex begins at unsteady state. The p-value becomes larger than 0.05 from 4th apex and afterward. In conclusion, from the analysis of Bartlett's test, the apexes reach the steady state after 4 hops.

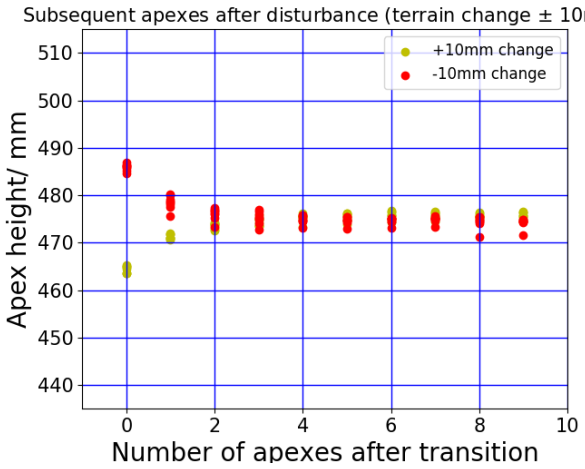

(a) ±10 mm terrain change after 0th apex

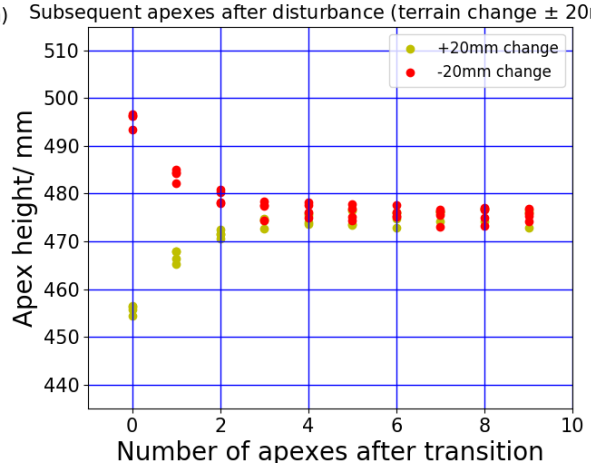

(b) ±20 mm terrain change after 0th apex

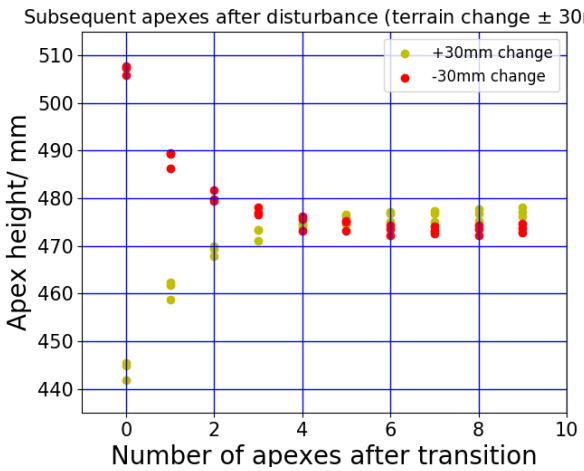

(c) ±30 mm terrain change after 0th apex

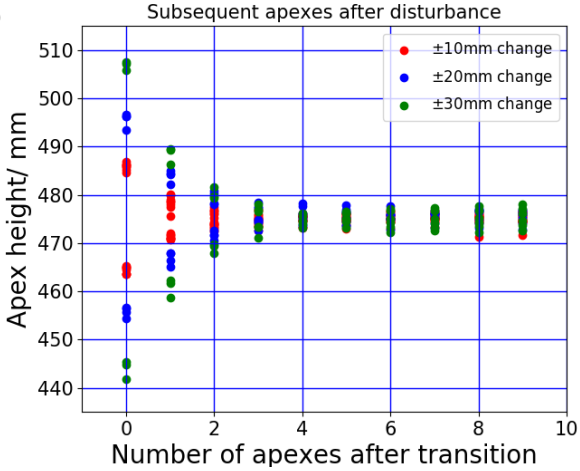

(d) all terrain change after 0th apex

Figure 4.4: Subsequent apexes after different terrain change, the terrain change happens after 0th apex

Chapter 5
DEADBEAT CONTROLLER

With the dynamic of the hopper detected, the system is asymptotically converge the steady apex height after the terrain disturbance within 30 mm. In this chapter, the controller is designed in section 5.1 based on mathematical theory to physical measurement. With the controller built, the validating experiment is conducted in section 5.2, which includes the experiment method, experiment result and result analysis.

5.1 Deadbeat Controller

The work of [9] has mathematically proven the deadbeat controller with Poincaré return map by implicit function theorem. In this section, one deadbeat controller for this psychical hopper is designed, whose mathematical model is not well determined. Utilizing the return map measured in subsection 5.1.2 and 5.1.3, a controller is generated which is designed to behave deadbeat.

5.1.1 Mathematical Method

In periodic running, Poincaré return map is applied to help analyze the hybrid system with in many studies [31, 32, 2, 8]. The state p in this system is the vertical position y and velocity $\dot{y}$ of the top marker, which stands for the vertical position and velocity of the COM. The lower dimension we choose as Poincaré section is apex section where the vertical position y reaches maximum and velocity $\dot{y} = 0$. The state of kth apex is $p_k = (y_k, \dot{y}_k) = (h_k, 0)$, the h_k is the kth apex height. And Poincaré map returns the next state in apex section,

$$P(p_k) = P((h_k, 0)) = p_{k+1} = (h_{k+1}, 0) \tag{5.1}$$

In section 4.1 by hopping without disturbance experiment, the system is known with stable apex height, which has variance under 1 mm. So a nominal apex height h_0 is set, and the return function is

$$P(p_k) = P((h_0, 0)) = p_{k+1} = (h_0, 0) \tag{5.2}$$

The terrain's disturbance Δs, which is input in the hopping system at touchdown, will cause the new apex state

$$P(p_k, \Delta s) = (h_0 + \Delta h_{\Delta s}, 0) \tag{5.3}$$

$\Delta h_{\Delta s}$ is the apex change cause by terrain's disturbance. Similarly, a control u during the hop will cause the output change Δh_u

$$P(p_k, u) = (h_0 + \Delta h_u, 0) \tag{5.4}$$

To reject the disturbance of Δs to the apex, the control u during the hop is set to achieve the goal

$$P(p_k, \Delta s, u) = (h_0 + \Delta h_{\Delta s} + \Delta h_u, 0) = (h_0, 0) \tag{5.5}$$

and we can get

$$\Delta h_{\Delta s} + \Delta h_u = 0. \tag{5.6}$$

With return map

$$f_1 : \Delta s \to \Delta h_{\Delta s}, f_2 : u \to \Delta h_u, \tag{5.7}$$

a solution of control u to function 5.6 is achieved given Δs, which can be expressed as

$$f_3(s) = u. \tag{5.8}$$

Here we get the mathematical solution of the deadbeat controller.

5.1.2 Terrain change -apex map

With the experiment result in section 4.2, the map of terrain change Δs to apex height change $\Delta h_{\Delta s}$ is obtained. In Fig 5.1, an approximate linear relationship is used to simplify

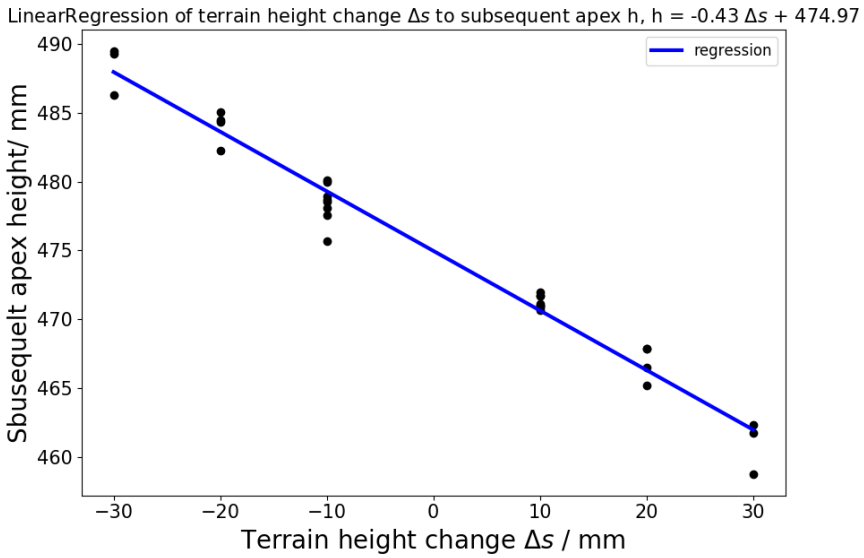

Figure 5.1: The $\Delta s - h$ map. A linear regression is applied for the interpretation of this relationship between Δs and h, in this regression the correlation coefficient is $r^2 = -0.9881$

the law between terrain disturbance Δs and subsequent apex height h. The variance of terrain height linearly changes the gravitational potential energy of the hopper to ground surface, while the apex height is also linear to the mechanical energy of the hopper. And the nominal apex $h_0 = 474.97$ mm.

5.1.3 Kp - apex map

There are many choices for the object of controller in running locomotion, in [9] the leg length is utilized as the feedforward controller to reject disturbance of the terrain height; the 'swing-leg retraction' observed by [32] used constant leg's swinging angular velocity in the SLIP model to simulate bipedal running, which matches terrain height to angle of attack. Studies in human's leg stiffness [35, 21] revealed the change of leg stiffness according to different terrains. In our 1-dimensional hopper, changing the hopper's 'stiffness' is an easier approach which can be achieved by setting proportional value of the PD control K_p when comparing

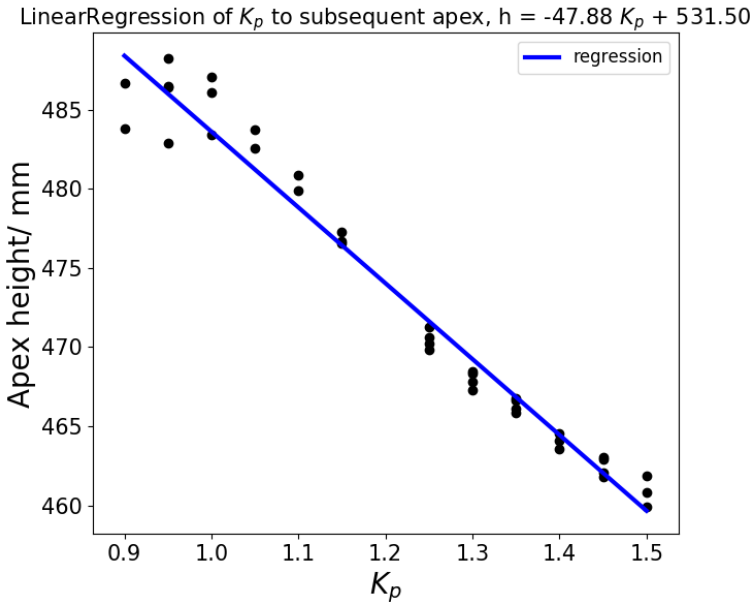

Figure 5.2: The $K_p - h$ map. A linear regression is applied for the interpretation of this relationship between K_p and h, in this regression the correlation coefficient is $r^2 = -0.9853$

with changing the physical configuration of the leg length. With the nadir detection hopping (Algorithm 3), after touchdown, a straightforward way to change the proportional parameter is to vary the K_p at extending position commanding. During extending position period, the leg is extended from the ground with energy injected to the upper body, and different K_ps during this period add different energy and finally the hopper achieves different apex heights.

The experiment of creating the K_p - apex h map is conducted, which measures the apexes at different K_ps in extend position. In Fig 5.2, the changing law of K_p and subsequent apex height h is simplified as a linear function.

With the return map $\Delta s - h$ and $K_p - h$, a K_p controller could be built with equation 5.6:

$$f_3 : K_p = 1.18 - 0.0089\Delta s. \tag{5.9}$$

5.2 Experimental validation of deadbeat controller

A K_p controller is built in Section 5.1, and in this section, this controller is validated by experiment.

5.2.1 Experiment method

In equation 5.9, the controller output comes from the disturbance input Δs. The experiment is conducted based on the hardware connection in Fig **??**. To detect the terrain height change Δs, the terrain's information s is reported from test bed's motor by USB serial port, meanwhile the motion capture camera detects the vertical position y at apex point. Finally $\Delta s = y - s - h_0$. The real time SDK of Qualysis camera enables the position capture in 100 Hz for apex detecting, and same terrain in section 4.2 is used in this validating experiment to compare the result with and without controller.

5.2.2 Result analysis

Fig 5.3 plots the result sorted by terrain change. Comparing to the open loop's result in Fig **??**, a faster speed of converging to stable state is achieved in Fig **??**, as the scattered apexes start to converge to the h_0 at 2th apexes for all terrain changes Δs.

Table 5.1: Statics of apexes height h in number of hop after terrain transition with K_p controller: mean $\bar{h}$, squared deviation σ, p-value of Bartlett test

number of hops	0	1	2	3	4	5	6	7	8	9
$\bar{h}$/ mm	474.9	474.1	474.8	474.6	474.8	474.7	474.9	474.7	474.7	474.6
σ/mm	15.9	3.9	1.4	1.0	1.0	0.8	0.8	0.9	0.9	1.4
p-value	1e-9	7e-6	0.70	0.31	0.40	0.92	0.30	0.76	0.68	0.79

Table 5.1 shows the statistical analysis from the validation experiment. Following the same principle of section 4.2 in analyzing the open loop, the variance of subsequent apexes

shrinks faster than the open loop (K_p controller takes 2 hops to have σ under 1.5 mm, while open loop costs 2 more hops in table 4.1). P-values from Bartlett test also indicates the apexes reaches the steady state at 2nd hop where p-value starts larger than 0.05.

Based on the experiment result of k_p controller and the comparison of apex change after disturbance between open loop and K_p controller, the conclusion could be reached that this K_p controller decreases the time for the hopper to achieve new steady apex after terrain's disturbance in the range of 30 mm.

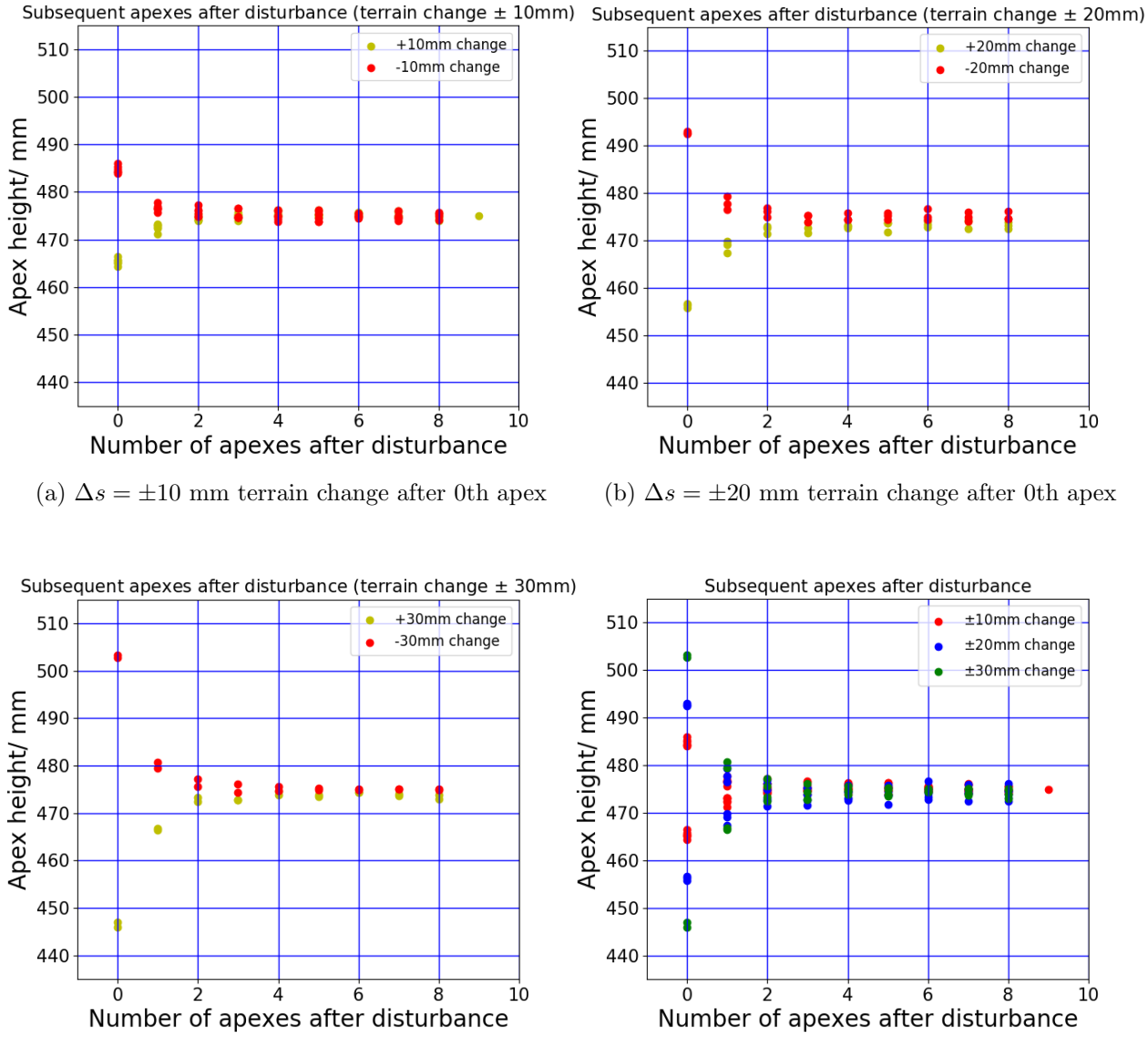

(a) $\Delta s = \pm 10$ mm terrain change after 0th apex

(b) $\Delta s = \pm 20$ mm terrain change after 0th apex

(c) $\Delta s = \pm 30$ mm terrain change after 0th apex

(d) all terrain change after 0th apex

Figure 5.3: Subsequent apexes after different terrain change, the terrain change happens after 0th apex

Chapter 6

CONCLUSION AND FUTURE WORK

6.1 Conclusion

This master thesis is aimed to use experimental method to validate a deadbeat controller on running locomotion. The control object is an 1-dimensional hopper. In this thesis work, three main parts are accomplished to achieve the thesis goal.

First, a test bed setup is designed, fabricated and tested for the simulation of uneven terrain under the hopper. A horizontal platform is designed with chain transmission to move the terrain on the platform. The test bed is controlled by motor's PD positioning command, which is able to move from one terrain position to another during the time the hopper is in the air so that no horizontal disturbance is caused by the terrain transition.

Second, the dynamics of the hopper is explored under terrain disturbance. To decrease the energy dissipation cause by impact to ground, a spring is attached between the leg. A hopping pattern with nadir detect is applied on the hopper to reject the unstable hopping caused by terrain disturbance. The terrain disturbing experiment includes the visual capture of hopper's position and open loop hopping with motor control. The result shows that hopper has the trend to converge to nominal apex height after terrain disturbance, which takes 4 hops before reaching new steady state within 30 mm change of terrain height. And a linear function is used to interprete the law of terrain height change Δs to subsequent apex h.

Third, the controller is designed to achieve the goal of rejecting the disturbance of terrain change. The proportional parameter in PD control K_p is chosen as the variable of the controller. By varying K_p, a Poincaré return map is built with control input on the apex section. The controlling function is obtained by integrating disturbance return map and control return map. Validation experiment of the controller shows that less hops are spent

after same disturbance for the controller to achieve new steady state than open loop hopping. Thus the conclusion is safely achieved by experimental validation that the controller increase the stability of the hopper to keep constant apex under disturbance. While the controller cannot achieve one step stable in [9], it makes the hopper deadbeat within certain arrange of disturbance and speeds up the procedure to become deadbeat.

6.2 Future work

With the result shown, we can this experimental validation could be improved in many aspects.

1. Increase the disturbance range In this experiment, the terrain's disturbance is ± 30 mm and the hopper's hopping height is around 140 mm. With consideration of limitation of physical configuration of the platform and hopping height, the following points help increase the disturbance range:

   i). A bigger horizontal platform will provides more space for different terrains;

   ii). The hopper's hopping height is related to the motor's power. The higher the hopping height, the larger range will the terrain have. The method to increasing hopping height includes applying more powerful motor, optimizing the hopping parameters (commanding position, proportional and derivative parameter in PD controller).

2. Achieve one-hop stability From the experiment result, the K_p controller cannot achieve steady state within on hop, reasons including the method to build the return map. Linearization is a simple but not most precise method in regression while we assume the range of regression is 'local'. And assuming the change of Δs and K_p is independent is not precise, a better mapping should be creating the map $P(x_k, (\Delta s, K_p) = x_{k+1}$, which requires larger experimental work for measurement.

3. Deeper exploration This controller's object is 1-dimensional hopping, while in future

the exciting application of deadbeat running controller includes 1-dimensional sagittal SLIP model, biped and multiped robots.

Chapter 7

APPENDIX A

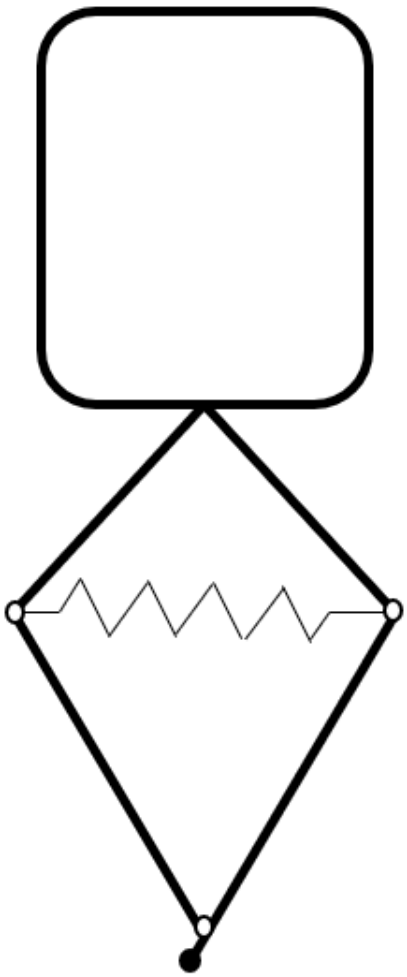

Figure 7.1: A linear spring attaches between two knees of the leg

BIBLIOGRAPHY

[1] Richard Altendorfer, Ned Moore, Haldun Komsuoglu, Martin Buehler, HB Brown, Dave McMordie, Uluc Saranli, Robert Full, and Daniel E Koditschek. Rhex: A biologically inspired hexapod runner. *Autonomous Robots*, 11(3):207–213, 2001.

[2] M Mert Ankarali and Uluç Saranli. Stride-to-stride energy regulation for robust self-stability of a torque-actuated dissipative spring-mass hopper. *Chaos: An Interdisciplinary Journal of Nonlinear Science*, 20(3):033121, 2010.

[3] MM Ankarali, O Arslan, and U Saranli. An analytical solution to the stance dynamics of passive spring-loaded inverted pendulum with damping. In *Mobile Robotics: Solutions and Challenges*, pages 693–700. World Scientific, 2010.

[4] Minoru Asada. Preface. *Adv. Robot.*, 10(2):139–142, January 1995.

[5] J. Baldassini. *An Examination of the Effects of Deformable Foam Contact Surfaces on Robotics Locomotion*. University of Washington, Seattle, WA, USA, 2017.

[6] Albrecht Bertram. *Understanding mammalian locomotion: concepts and applications*. John Wiley & Sons, 2016.

[7] Reinhard Blickhan and RJ Full. Similarity in multilegged locomotion: bouncing like a monopode. *Journal of Comparative Physiology A*, 173(5):509–517, 1993.

[8] Sean G Carver, Noah J Cowan, and John M Guckenheimer. Lateral stability of the spring-mass hopper suggests a two-step control strategy for running. *Chaos: An Interdisciplinary Journal of Nonlinear Science*, 19(2):026106, 2009.

[9] G Council, S Yang, and S Revzen. Deadbeat control with (almost) no sensing in a hybrid model of legged locomotion. In *Proceedings of the 2014 International Conference on Advanced Mechatronic Systems*, pages 475–480, August 2014.

[10] Monica A Daley and Andrew A Biewener. Running over rough terrain reveals limb control for intrinsic stability. *Proceedings of the National Academy of Sciences*, 103(42):15681–15686, 2006.

[11] Péter Fankhauser, Marko Bjelonic, Dario Bellicoso, Takahiro Miki, and Marco Hutter. Robust rough-terrain locomotion with a quadrupedal robot. In *IEEE International Conference on Robotics and Automation (ICRA 2018)*. ETH Zurich, 2018.

[12] Claire T Farley and Daniel P Ferris. 10 biomechanics of walking and running: Center of mass movements to muscle action. *Exercise and sport sciences reviews*, 26(1):253–286, 1998.

[13] Robert J Full and Daniel E Koditschek. Templates and anchors: neuromechanical hypotheses of legged locomotion on land. *Journal of experimental biology*, 202(23):3325–3332, 1999.

[14] Raffaele M Ghigliazza, Richard Altendorfer, Philip Holmes, and D Koditschek. A simply stabilized running model. *SIAM review*, 47(3):519–549, 2005.

[15] Rafal Goebel, Ricardo G Sanfelice, and Andrew R Teel. Hybrid dynamical systems. *IEEE Control Systems*, 29(2):28–93, 2009.

[16] Aaron M Johnson, Samuel A Burden, and Daniel E Koditschek. A hybrid systems model for simple manipulation and self-manipulation systems. *The International Journal of Robotics Research*, 35(11):1354–1392, 2016.

[17] Thomas Kailath. *Linear systems*, volume 156. Prentice-Hall Englewood Cliffs, NJ, 1980.

[18] G Kenneally, A De, and D E Koditschek. Design principles for a family of Direct-Drive legged robots. *IEEE Robotics and Automation Letters*, 1(2):900–907, July 2016.

[19] G Kenneally and D E Koditschek. Leg design for energy management in an electromechanical robot. In *2015 IEEE/RSJ International Conference on Intelligent Robots and Systems (IROS)*, pages 5712–5718, 2015.

[20] Sami Kuitunen, Paavo V Komi, and Heikki Kyröläinen. Knee and ankle joint stiffness in sprint running. *Medicine and science in sports and exercise*, 34(1):166–173, 2002.

[21] Jakob Lorentzen, Maria Willerslev-Olsen, Helle Hüche Larsen, Christian Svane, Christian Forman, Rasmus Frisk, Simon Francis Farmer, Uwe Kersting, and Jens Bo Nielsen. Feedforward neural control of toe walking in humans. *The Journal of physiology*, 2018.

[22] K Maekawa, T Obikawa, Y Yamane, and T H C Childs. *Mechanical Design*. Elsevier, December 2003.

[23] Matthew Millard, Eric Kubica, and John McPhee. Forward dynamic human gait simulation using a slip target model. *Procedia IUTAM*, 2:142–157, 2011.

[24] Gill A Pratt and Matthew M Williamson. Series elastic actuators. In *Intelligent Robots and Systems 95.'Human Robot Interaction and Cooperative Robots', Proceedings. 1995 IEEE/RSJ International Conference on*, volume 1, pages 399–406, 1995.

[25] Marc Raibert, Kevin Blankespoor, Gabriel Nelson, and Rob Playter. Bigdog, the rough-terrain quadruped robot. *IFAC Proceedings Volumes*, 41(2):10822–10825, 2008.

[26] Aida Mohammadi Nejad Rashty, Maziar Ahmad Sharbafi, and Andre Seyfarth. Slip with swing leg augmentation as a model for running. In *Intelligent Robots and Systems (IROS 2014), 2014 IEEE/RSJ International Conference on*, pages 2543–2549. IEEE, 2014.

[27] C David Remy. *Optimal exploitation of natural dynamics in legged locomotion*. PhD thesis, ETH Zurich, 2011.

[28] A M Schillings, B M Van Wezel, and J Duysens. Mechanically induced stumbling during human treadmill walking. *J. Neurosci. Methods*, 67(1):11–17, July 1996.

[29] Justin E Seipel and Philip Holmes. Running in three dimensions: Analysis of a point-mass sprung-leg model. *The International Journal of Robotics Research*, 24(8):657–674, 2005.

[30] S Seok, A Wang, Meng Yee Chuah, D Otten, J Lang, and S Kim. Design principles for highly efficient quadrupeds and implementation on the MIT cheetah robot. In *2013 IEEE International Conference on Robotics and Automation*, pages 3307–3312, May 2013.

[31] Andre Seyfarth, Hartmut Geyer, Michael Günther, and Reinhard Blickhan. A movement criterion for running. *Journal of biomechanics*, 35(5):649–655, 2002.

[32] André Seyfarth, Hartmut Geyer, and Hugh Herr. Swing-leg retraction: a simple control model for stable running. *Journal of Experimental Biology*, 206(15):2547–2555, 2003.

[33] G Snedecor and W Cochran. Stadistical methods. eight ed. ames, 1989.

[34] Y. Sosnovskaya. *External Measurement System for Robot Dynamics*. University of Washington, Seattle, WA, USA, 2017.

[35] Alexandra S Voloshina and Daniel P Ferris. Biomechanics and energetics of running on uneven terrain. *Journal of Experimental Biology*, 218(5):711–719, 2015.

[36] Alexandra S Voloshina, Arthur D Kuo, Monica A Daley, and Daniel P Ferris. Biomechanics and energetics of walking on uneven terrain. *J. Exp. Biol.*, 216(Pt 21):3963–3970, November 2013.